Noise-induced synchronous stochastic oscillations in small scale cultured heart-cell networks*

Yuan Lan(袁 岚), Liu Zhi-Qiang(刘志强), Zhang Hui-Min(张慧敏), Ding Xue-Li(丁学利), Yang Ming-Hao(杨明浩), Gu Hua-Guang(古华光)†, and Ren Wei(任 维)

College of Life Science, Shaanxi Normal University, Xi'an 710062*, China*

(Received 8 April 2010; revised manuscript received 2 September 2010)

This paper reports that the synchronous integer multiple oscillations of heart-cell networks or clusters are observed in the biology experiment. The behaviour of the integer multiple rhythm is a transition between super- and sub-threshold oscillations, the stochastic mechanism of the transition is identified. The similar synchronized oscillations are theoretically reproduced in the stochastic network composed of heterogeneous cells whose behaviours are chosen as excitable or oscillatory states near a Hopf bifurcation point. The parameter regions of coupling strength and noise density that the complex oscillatory rhythms can be simulated are identified. The results show that the rhythm results from a simple stochastic alternating process between super- and sub-threshold oscillations. Studies on single heart cells forming these clusters reveal excitable or oscillatory state nearby a Hopf bifurcation point underpinning the stochastic alternation. In discussion, the results are related to some abnormal heartbeat rhythms such as the sinus arrest.

Keywords: synchronous oscillation, network, Hopf bifurcation, effect of noise, integer multiple rhythms, heart cell

PACS: 05.45.Xt, 87.19.Hh, 87.18.Tt, 87.18.Hf **DOI:** 10.1088/1674-1056/20/2/020508

1. Introduction

Pace-making rhythms of the heart are central to life,[1,2] but mechanisms of a great number of cardiac arrhythmia even leading to death are still unclear.[2−4] In recent years, studies on the origin and dynamics of normal and abnormal cardiac rhythms are growing rapidly, in which cultured networks of the heart cells served as the model system for both propagation mediums and pacemaker tissues.[5−8] According to purpose of the study, the cultured networks of heart cells with very different size were selectively employed. Large scale cultured networks of a continuous monolayer of cells were frequently used to study a variety of spatiotemporal patterns such as spiral waves and intrinsic beating variability,[5,6] whereas small scale networks composed of a cluster of cells have long been used to study synchronous pace-making rhythms (see Refs. [7], also see Ref. [8] and the references therein).

Small heart-cell networks, called clusters in physiology, are capable of not only spontaneous oscillations but also characteristic responses to external stimulation. In a series of pioneering studies, changes in oscillatory rhythm of the chick heart-cell aggregates in response to single-pulses and periodic stimulations were observed experimentally and predicted theoretically from mathematical analysis.[1,2,9,10] The works provide important implications for understanding of the normal and pathological behaviours in cardiac tissues. In previous studies, emergence of synchronous oscillations has been demonstrated to be originated from coupling between the spontaneously active heart cells within the cluster.[7,11−15] During the culture, neighbouring isolated dissolved cells may make contacts and establish gap junctions, and eventually become coupled together to form a synchronous cluster. Repetitive observations have shown that the oscillatory rhythm of several originally separated cells can eventually converge during the forming of gap junctions.[7,13,15]

It has been widely accepted that synchronous oscillation in a cluster is strongly associated with the number of its inclusive cells, the heterogeneity of these cells, and the coupling strength between these cells. The pattern of linkage in the cluster is usually considered as nearest-neighbour connections.[7,11−15] Varia-

*Project supported by the National Natural Science Foundation of China (Grant Nos. 10772101 and 30670533), the National High Technology Research and Development Program of China (Grant No. 2007AA02Z310) and the Fundamental Research Funds for the Central Universities (Grant No. GK200902025).

†Corresponding author. E-mail: guhuaguang@263.net

© 2011 Chinese Physical Society and IOP Publishing Ltd

tions in spontaneous oscillation of isolated heart cells, such as those in magnitude and phase and in inter-beat intervals, reflect heterogeneity of the cells. Interestingly, noise has also been proved to be effective in the generation of various oscillatory rhythms of isolated heart cells or heart-cell clusters. For example, a small perturbation of internal or external noise has been shown to be able to annihilate the rhythmic beating of heart cells by forcing them from a limited cycle oscillation to a resting steady state.[1,2,16] Fluctuations in inter-beat interval of rhythmic oscillations of heart-cell clusters were also ascribed to be caused by internal noise and inversely related to the number of the inclusive cells.[7] Such effects of noise might be important in the generation of complex pathological heart rhythms. The excitable state of the excitable systems, such as excitable media, network and single cells, has been given much attention in the studies about roles of noise.[17] For a unit in the excitable system or media, such as single neurons or heart cells, the excitable state can be related to the bifurcation from stable equilibrium point to limited cycle in nonlinear dynamics,[18] including the Hopf bifurcation point from the stable focus to the limited cycle and the saddle-node bifurcation from the stable node to the limited cycle. The behaviour is changed from quiescent state to oscillating state correspondingly. The excitable state is the quiescent state near the bifurcation point. If the distance of the excitable state is closer to the bifurcation point, the system is easier to become excited state or oscillation correspondingly.[18]

Interplay between internal or external noise and the concerned system's dynamics at excitable state has been always an important issue in physics as well as in biology.[19] Many studies have shown that noise may play positive roles in information processing in both sensory nerve terminals and neuronal populations through its interplay with the bifurcation dynamics of the neuronal systems.[20−24] The relevant physical process is associated with stochastic resonance (SR)[4,25] or coherence resonance (CR).[26] In the case of SR or CR phenomenon, dynamic noise is able to induce various stable stochastic neural firing rhythms, many such noise-induced neuronal firing trains can be characterized by integer multiple properties in their inter-spike intervals.[22−24] However, dynamic effects of noise in generation of spontaneous oscillatory rhythms in heart cells or network are still rarely studied.[27−29] Whether SR or CR phenomenon is effective in oscillations of cardiac pace-making tissues or not is also an unaddressed interesting question.

The rhythms of cardiac cells are exhibited in three aspects, membrane potential,[1,2,9,10] intracellular calcium concentration ($[Ca^{2+}]_i$)[4,30−32] and beating of cardiac muscle.[33] The three rhythms are generated in sequence when an action potential is generated. The rhythm of membrane potential, containing physiological significance in both time and amplitude, can be recorded in single cells by patch clamp. The rhythms of $[Ca^{2+}]_i$ can be simultaneously achieved in multiple cells in a network and are always used to study the spatiotemporal pattern of multiple cells.[4,30−32] The beating rhythm only reflects time interval of continuous beatings of single cells or multiple cells in a network as a whole.[33] In the experiment reported in this paper, when the rhythms of different cells in the network are studied, the rhythms of $[Ca^{2+}]_i$ are employed. When the rhythms of single cells are studied, the rhythms of membrane potential are recorded. While in the theoretical studies, the rhythms of membrane potential are simulated, whether in the network or single cells. It is because the rhythms of the network or single cells are the focus of this paper.

In the present paper, we observed the oscillatory rhythms generated by dissolved single heart cells and those by small heart-cell clusters. We particularly studied a series of integer multiple rhythms generated by small heart-cell clusters. Formation of such synchronous integer multiple oscillations were related to heterogeneity of the inclusive cells. The experimentally observed integer multiple oscillations were reproduced in mathematical modeling and explained with a CR effect resulting from interplay between internal noise and the dynamics of excitable state or oscillation near a Hopf bifurcation. The rest of the present paper is organized as follows. Section 2 is materials and methods. Section 3 introduces experimental observations of the integer multiple oscillations in small heart-cell clusters. Section 4 provides patch clamp recording of excitatory rhythms of single heart cells. Section 5 is the numerical simulation of the experimental result of single heart cells. Section 6 is the theoretical prediction of the integer multiple oscillations of heart-cell clusters. An analysis of the effects of noise on the excitable or oscillation state near the Hopf bifurcation is also given in Sections 5 and 6. Section 7 includes the discussion and conclusion.

2. Experimental methods and data analysis methods

Heart cells were prepared from 1- to 2-day old neonatal Wistar rats. The ventricles were removed after decapitation and rinsed with Dulbecco's Modified Eagle's Medium (DMEM). They were then minced into fragments and digested in phosphate buffer solution (PBS) with 0.1% collagenase and 0.2% ethylene glycol tetraacetic acid (EGTA). The digestion was terminated by PBS with serum and the digested fragments were centrifuged at 1000 revolutions per minute (rpm) for two minutes. The precipitated cell components were suspended in DMEM. The heart cells were separated from fibroblast by selective adhesion methods and plated onto petri dishes at a density of 5×10^5 cells/mL. The isolated heart cells were cultured at 37 °C with 5% CO_2 and 95% O_2 for 3–7 days during which neighbouring cells established connections and thus formed small clusters. In the present study, only those small clusters containing 3–6 cells were used to perform calcium imaging observation. The cultured clusters were loaded with the fluorescent Ca^{2+} indicator 60 μmol/L Fura-2/Acetoxymethy (AM) (Sigma, America) for 40–50 min and then washed with PBS and DMEM buffered with 5 mmol/L PBS containing 10% Fetal Bovine serum (FBS) for 10 min to allow for the de-esterification of the Fura-2/AM. Cells were visualized on the inverted microscope (Zeiss, Germany) equipped with a Plan-Neofluar 20×0.75NA (Zeiss, Germany) objective. Fluorescence was detected with a charge coupled device (CCD) camera (PCO, Germany). In each observation, pairs of the fluorescence intensity excited at 340-nm and 380-nm were captured every 62 ms using an emission wavelength of 510 nm. Consecutive images were recorded in a computer and analysed off-line. Intracellular calcium concentration ($[Ca^{2+}]_i$) was estimated from the ratio of the 340-nm and 380-nm imagines.

Curves of $[Ca^{2+}]_i$ impulses versus time were obtained by calculated average fluorescence intensity of ratio in selected areas through the consecutive images. When calcium oscillation in a cluster is observed, an area of interest is selected for each cell in this cluster and, therefore, number of traces in Figs. 1(a) and 1(b) indicates the number of cells in the observed cluster while wave form of the traces shows temporal evolution of the oscillation.

In order to study transitions between the integer multiple and regular oscillation rhythms, patch clamp (Axon700B, USA) was employed to record the rhythms of a cell in the clusters. Membrane voltage oscillation of one cell of the synchronous clusters was recorded by using a microelectrode attached on the cell surface to perform current-clamp manipulation. Once a spontaneous voltage oscillation (action potential train) exhibiting the integer multiple characteristics is observed, current injection is then applied to induce the possible pattern transition procedure.

Synchronization between the traces was characterized by correlation coefficients, phase difference and timing of the calcium oscillatory peaks. The phase of a signal $x(t)$ was acquired by using Hilbert transformation.

$$x_h(t) = \frac{1}{\pi}\int_{-\infty}^{+\infty}\frac{x(\tau)}{t-\tau}\mathrm{d}\tau, \tag{1}$$

where improper integral was understood in terms of its Cauchy principal value. After the Hilbert transformation, an analytical signal yields

$$S(t) = x(t) + \mathrm{i}\, x_h(t) = A(t)\exp(\mathrm{i}\,\phi(t)), \tag{2}$$

where $\mathrm{i}^2 = -1$, $A(t)$ is the amplitude, and $\phi(t)$ is the phase of $x(t)$.

In addition, cross-correlation coefficient (CC) between two signals was also employed to describe the synchronization. Cross-correlation coefficient between two times series signals $x(j)$ and $y(j)$ (j = 1, 2, ..., M) is as follows:

$$CC = \frac{\sum_{j=1}^{M}(y(j)-\bar{y})(x(j)-\bar{x})}{\sqrt{\sum_{j=1}^{M}(y(j)-\bar{y})^2\Sigma_{j=1}^{M}(x(j)-\bar{x})^2}}, \tag{3}$$

where $\bar{x}$ and $\bar{y}$ are the mean of $x(j)$ and $y(j)$ (j = 1, 2, ..., M). The CC yields a value between 0 and 1. Synchronization between the two signals leads to higher values of CC.

The non-periodic deterministic property of a chaotic time series or stochastic property of a stochastic time series can be estimated by computing the normalized prediction error (NPE). In this paper, the simple nearest-neighbour method[19] was used and the algorithm is described below.

With reconstruction dimension m, the entire time series was transformed into N state points in reconstructed space R_m. For a given point $V_0 = (t_{i_0}, \ldots, t_{i_0-m+1})$ in R_m, bN (b is constant and less than 1) points nearest to V_0 were chosen and recorded as $U_l = (t_{j_l}, \ldots, t_{j_l-m+1})$ ($1 \le l \le bN$). The average $p_{j_0} = \frac{1}{bN}\sum_{l=1}^{bN} t_{j_l+h}$ was used to approximate future value of t_{i_0+h}. The difference $p - t_{i_0+h}$ was the h step

prediction error at V_0. For all state points, the normalized prediction error (NPE) is defined as

$$\mathrm{NPE} = \frac{\langle (p_{i_0} - t_{i_0+h})^2 \rangle^{1/2}}{\langle (\bar{t} - t_{i_0+l})^2 \rangle^{1/2}}, \tag{4}$$

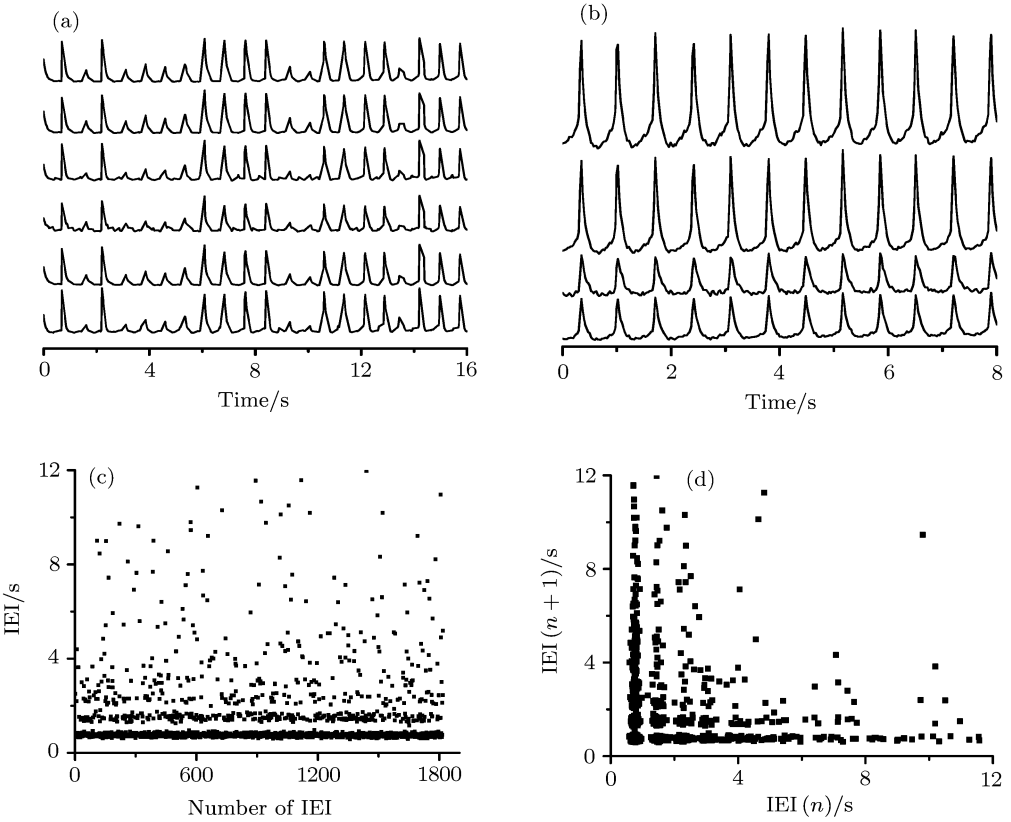
where $\bar{t}$ is the average of the time series and $\langle \bullet \rangle$ stands for the average over the time series. From the definition, a value of NPE much less than 1.0 means that there is linear or nonlinear predictability in the time series beyond the baseline prediction of the series mean.

NPE value of the original chaotic time series is much less than 1 in a short term of prediction and approaches 1 in a long term, while that of stochastic time series is always nearly 1.

3. Synchronous integer multiple rhythms in small heart-cell networks

In our experiment, the synchronous calcium oscillations in heart-cell clusters exhibit various temporal patterns. In the present study, we particularly introduced the clearly distinguished integer multiple rhythms in 19 of the 71 totally observed clusters. As an example of the integer multiple rhythm, the intracellular calcium traces of all the six cells forming a cluster are shown in Fig. 1(a). In contrast with the regular oscillation of a cluster with 4 cells shown in Fig. 1(b), this integer multiple rhythms is formed by regular oscillation interspersed occasionally with small subthreshold oscillations and thus have a random appearance. Estimation using the above described measures indicates that the calcium oscillations of the different cells in a same cluster are highly synchronous. For example, CC between any two of the 6 traces in Fig. 1(a) is bigger than 0.95. Mean of phase-difference between any two traces is less than 0.17.

In order to analyse the dynamic property of such integer multiple oscillations, we defined one superthreshold oscillation as an event and the interval between two successive events as inter-event interval (IEI), and then transform the original calcium oscillation traces into IEI series. The IEI values in such IEI series are always approximately as multiple times of a basic value. The first return map of such IEI series exhibits a lattice-like structure and the IEI histograms (IEIH) manifest a multi-peak distribution showing an exponential decay in amplitude of the peaks, indicating that the observed oscillatory pattern may result from a stochastic transition process.



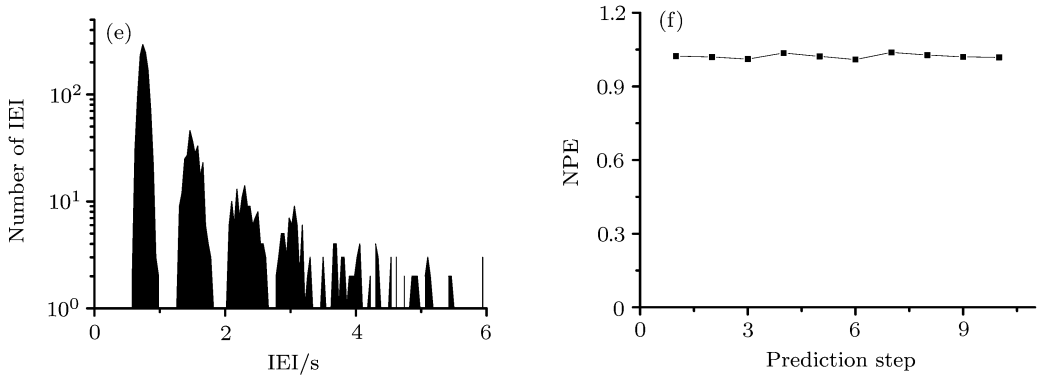


Fig. 1. Calcium oscillation in heart-cell clusters: (a) stochastic rhythms of calcium concentration of 6 cells in a heart-cell cluster; (b) regular rhythms of calcium concentration of 4 cells in a heart-cell cluster; (c) inter-event interval (IEI) series of (a); (d) first return map of the IEI series of (a); (e) IEI histogram of (a); (f) nonlinear prediction of IEI series of (a).

Estimation with nonlinear measures such as NPE and autocorrelation coefficient also suggests a stochastic dynamics of the oscillations. As an example, the IEI times series, its first return map, and its IEIH transformed from one trace of calcium oscillation shown in Fig. 1(a) are illustrated in Figs. 1(c), 1(d), and 1(e), respectively. The NPE of the IEI series is nearly 1, suggesting that the IEI series may result from a stochastic dynamics, as shown in Fig. 1(f).

In 6 clusters, depolarizing manipulation induced a transition from the integer multiple rhythm to the regular rhythm, whereas hyperpolarization induced a transition to subthreshold oscillation, suggesting that the integer multiple oscillation may be an intermediate activity between resting and regular oscillation. An example of such transition is shown in Fig. 2. Membrane potential oscillation of a cluster was able to be changed from the integer multiple rhythm (injection current $I = 0$ pA, Fig. 2(a)) either to a regular rhythm ($I = 100$ pA, Fig. 2(b)) or to a subthreshold oscillation ($I = -100$ pA, Fig. 2(c)).

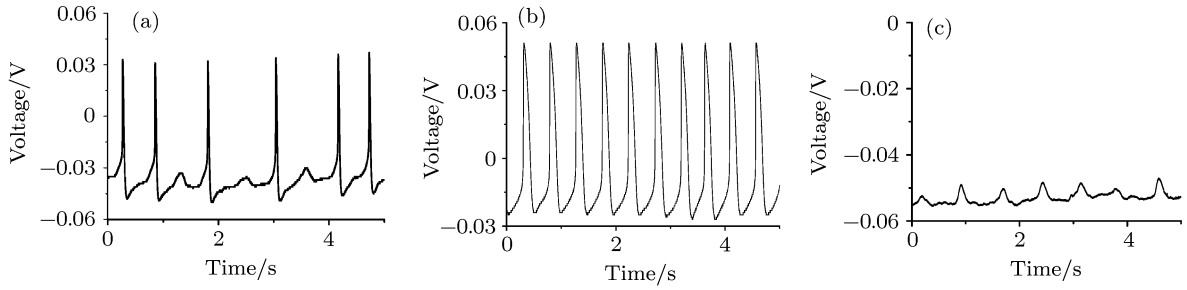


Fig. 2. Transition procedure in oscillation in a heart-cell cluster: (a) stochastic rhythms when injection current $I = 0$ pA; (b) regular rhythms when $I = 100$ pA; (c) subthreshold oscillation when $I = -100$ pA.

4. Experimental observation of integer multiple rhythms on single heart cells

In experiments introduced in Section 2, both regular and integer multiple rhythms were observed in synchronous calcium oscillation in the small clusters, in which the number of cells is 4–6 and the linkage can be reasonably regarded as nearest-neighbour connection. Therefore, we paid particular attention to the heterogeneity of the cells to study the origin of the different rhythms by observing membrane potential oscillatory patterns of single cells forming the clusters. In what follows, we first introduced the spontaneous regular and integer multiple firing patterns of single cells and then showed that current injection also induced oscillatory pattern transitions similar to what observed on heart-cell clusters.

A current clamp procedure[33] was applied to single cells cultured for 1–2 days to observe their spontaneous membrane voltage oscillations. The 54 observed cells exhibit stable spontaneous oscillatory trains. Among them, 31 cells display regular oscillations (Fig. 3(a)) and 5 cells display stable action potential trains in a rhythm very similar to the integer multiple rhythms observed in heart-cell clusters.

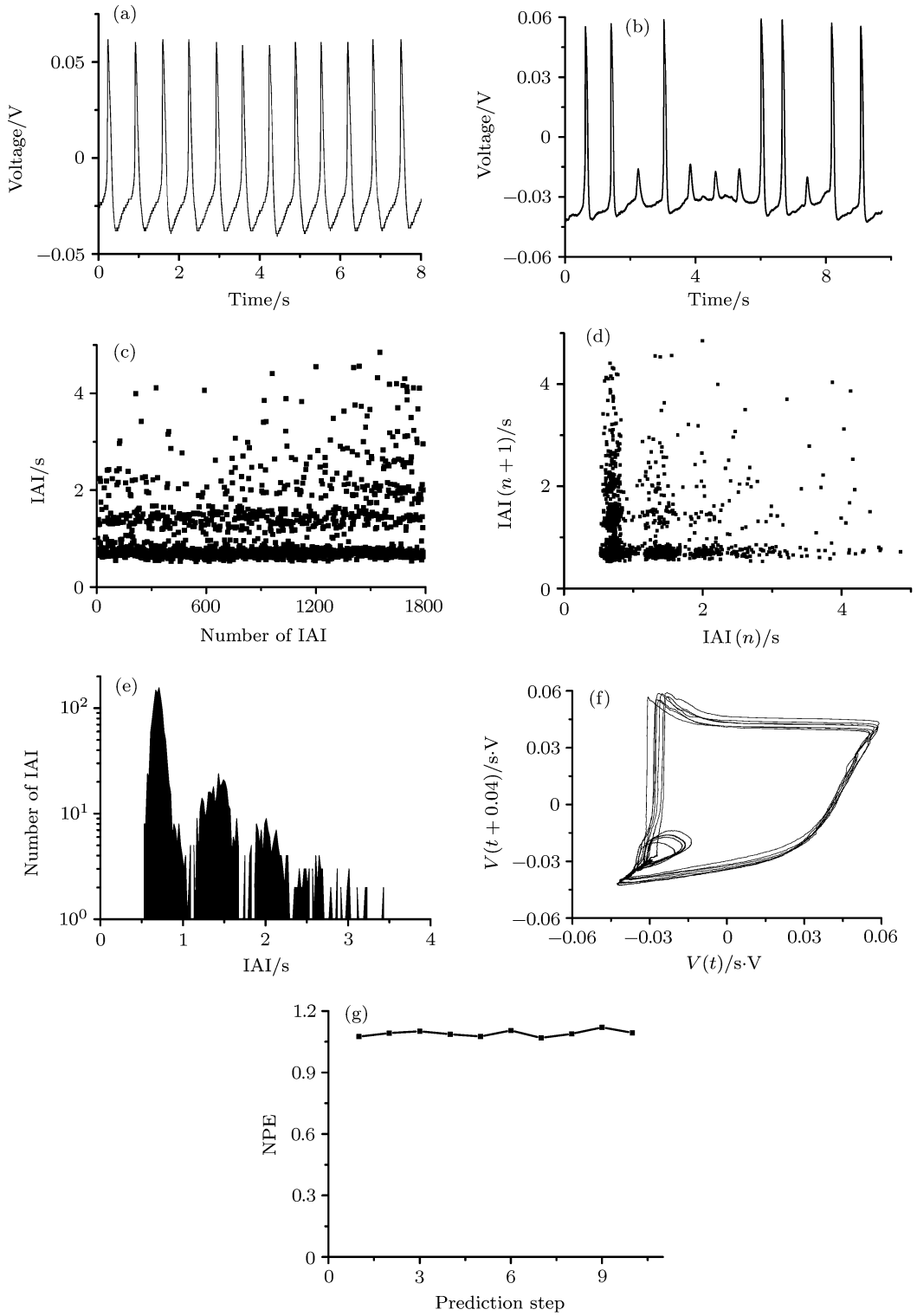


Fig. 3. Rhythm recorded in single cells: (a) regular rhythm; (b) stochastic integer multiple rhythm; (c) the IAI series of stochastic integer multiple rhythm; (d) first return map of IAI series; (e) IAI histogram; (f) delay coordinate portray of membrane voltage (delay is 40 ms); (g) nonlinear predication of the stochastic integer multiple rhythm.

As exemplified in Fig. 3(b)–3(f), in this integer multiple oscillations the regular action potential train is

interspersed with one or more cycles of subthreshold oscillations (Fig. 3(b)), the inter-action potential interval (IAI) series (Fig. 3(c)) also exhibits a lattice structure in its first return map (Fig. 3(d)) and an exponentially decaying multi-peak distribution in its IAI histogram (Fig. 3(e)). As shown in Fig. 3(f), the trajectories of sub- and super-threshold membrane voltage are clearly distinct in delay coordinate portray (the delay is 40 ms). Such characteristics suggest that the integer multiple oscillatory rhythm is stochastic and results from successive alternations between two trajectories, one is an action potential and the other is a subthreshold oscillation.

Also similar to what observed in heart-cell clusters, application of a polarizing inward current (+10 pA) or a hyperpolarizing outward current (−3 pA) induced a transition from an integer multiple oscillatory rhythm (Fig. 4(a)) to a regular rhythm (Fig. 4(b), $n = 4$) or a sub-threshold oscillatory state (Fig. 4(c), $n = 4$), respectively.

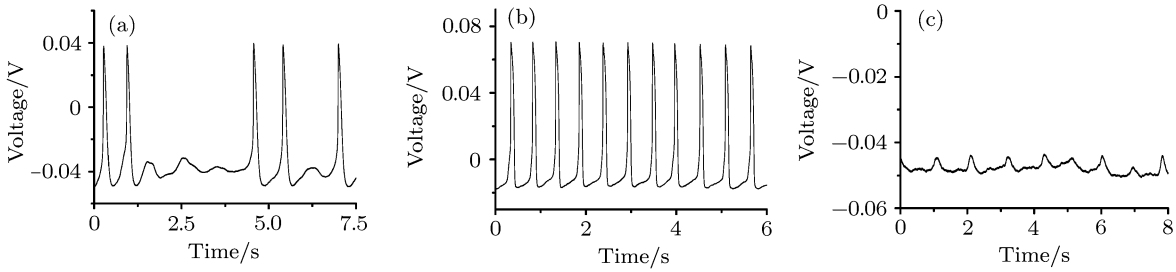


Fig. 4. Changes in the oscillatory rhythm of a single heart cell: (a) integer multiple oscillatory rhythm; (b) regular rhythm with application of depolarizing inward current (+10 pA); (c) sub-threshold oscillatory state with application of a hyperpolarizing outward current (−3 pA).

We further applied a ramp current on the single heart cells ($n = 5$) and observed a gradual transition procedure from sub-threshold oscillations to integer multiple oscillations, and finally to continual regular oscillations (in Fig. 5 the current from −30 pA to +10 pA in 240 s). This result indicates that the integer multiple oscillation of single heart cells is also an intermediate activity between resting and regular periodic oscillations.

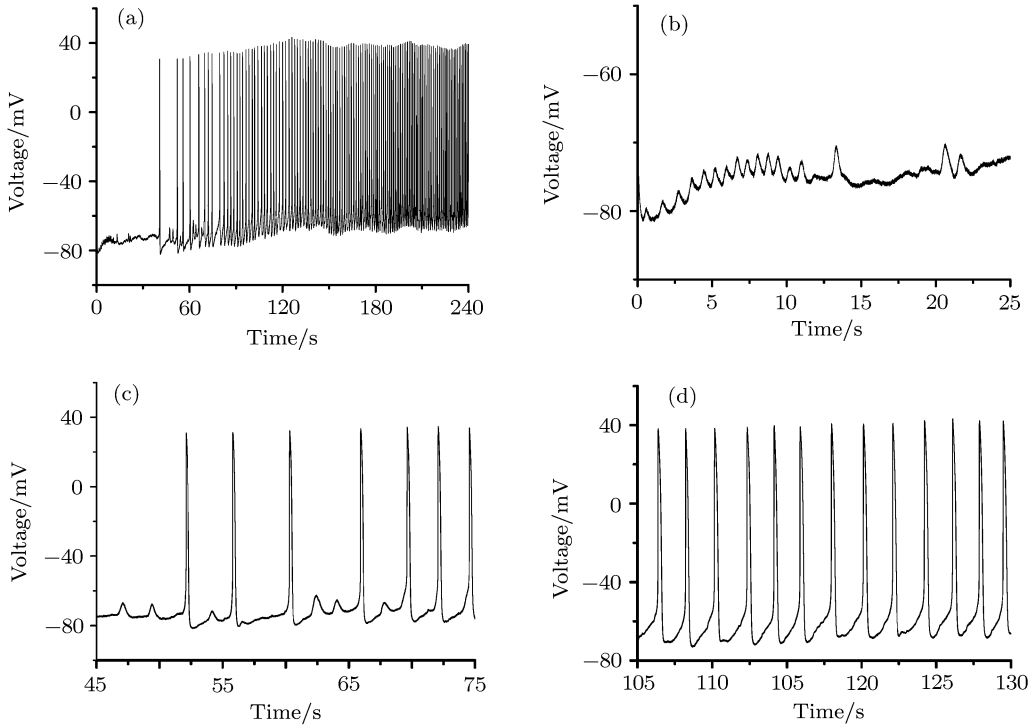


Fig. 5. (a) A gradual transition procedure from sub-threshold oscillation to integer multiple oscillation, and to regulation oscillation induced by a ramp current (from −30 pA to +10 pA in 240 s.) (b) Cyclic sub-threshold oscillation. (c) The action potential train interspersed by sub-threshold oscillation. (d) The regular action potential train.

The experimental results introduced in Sections 3 and 4 strongly suggest that the integer multiple oscillation is an intermediate activity between resting and regular super-threshold oscillation. This oscillatory pattern may result from the system's stochastic alternation between sub- and super-threshold trajectories. The stochastic characteristics also imply that the alternation is induced by the effect of noise. We then hypothesized that single heart cells with biological parameters such configured as the dynamics of their membrane oscillation nearby a Hopf bifurcation may generate integer multiple oscillations under the dynamical driven of internal noise, while those configured to be aparted from a Hopf bifurcation may be at rest or generate limited cycle oscillations. In small clusters like those employed in this study, heterogeneity of the heart cells may lead to different synchronous oscillations, clusters composed of cells nearby a Hopf bifurcation point may generate the synchronous integer multiple oscillations. In what follows we test for this hypothesis from theoretical simulation with an excitable cell model and its network.

5. Theoretical prediction for the integer multiple oscillations with a single cell model

Increasingly collected biological data have led to rather complicated models of heart-cells, some including more than ten ordinary differential equations and fifty parameters describing various ionic currents.[30,34,35] These models are specific to various heart cells and instructive to physiological studies on the dynamic functions of particular ion channels. In order to reveal generality, we seek a balance between such complex realistic models and simpler phenomenological ones like the van der Pol or FitzHugh–Nagumo oscillator.[13,36] Although similar results can be obtained with some other models containing more complex ionic components, we particularly chose the Morris–Lecar (ML) model[37] to explicitly explain the underpinning dynamics of our experimental observations. This model has been successfully employed to describe the pace-making dynamics of cardiac tissues.[12]

The ML model is described as follows:

$$\begin{aligned} C\frac{\mathrm{d}V}{\mathrm{d}t} &= -g_{\mathrm{Ca}}m_{\infty}(V-V_{\mathrm{Ca}}) - g_{\mathrm{K}}w(V-V_{\mathrm{K}}) \\ &\quad - g_{\mathrm{L}}(V-V_{\mathrm{L}}) + I, \end{aligned} \tag{5}$$

$$\frac{\mathrm{d}w}{\mathrm{d}t} = \phi\frac{(\omega_{\infty}-\omega)}{\tau_{\omega}}, \tag{6}$$

where t is the time (the independent variable). The dependent variables are V (the membrane potential) and ω (the activation of delayed rectifier K^+ current). The first equation contains calcium, potassium and leakage currents across the membrane of the cell. The explicit expressions for m_{∞}, ω_{∞} and τ_{ω} are

$$\begin{aligned} m_{\infty} &= 0.5\left(1+\tanh\left(\frac{V-V_1}{V_2}\right)\right), \\ \omega_{\infty} &= 0.5\left(1+\tanh\left(\frac{V-V_3}{V_4}\right)\right), \\ \tau_{\omega} &= 1/\cosh\left(\frac{V-V_3}{2V_4}\right). \end{aligned}$$

The I represents the injected current in patch clamp experiment on heart-cells. In the present study, the parameters are chosen as $C = 20$ μF, $V_{\mathrm{Ca}} = 120$ mV, $V_{\mathrm{K}} = -84$ mV, $g_{\mathrm{L}} = 2$ mS/cm^2, $V_1 = -1.2$ mV, $V_2 = 18$ mV, $V_3 = 2$ mV, $V_4 = 30$ mV, $V_{\mathrm{L}} = -67.9$ mV, and $\phi = 0.04$. The unit of the conductance is mS/cm^2.

A Gaussian white noise $\xi(t)$, reflecting the inevitable fluctuation in real cardiac cells, is introduced to Eq. (5) to form the stochastic ML model. The statistical properties of $\xi(t)$ is $\langle\xi(t)\rangle = 0$ and $\langle\xi(t)\xi(t')\rangle = 2D\delta(t-t')$, where D is the noise density, and $\delta(\cdot)$ is the Dirac δ-function. The deterministic and stochastic ML models as well as their networks are solved by Euler numerical integration method with integration time step being 0.1 s. Upstrokes of voltage reached the amplitude of 25.0 mV are counted as pulses.

Values of g_{Ca} and g_{K} are adjusted to reflect the heterogeneity of different cells. With g_{Ca} and g_{K} values varied in a reasonable parameter range, the cells might manifest either resting or limited cycle oscillations. The bifurcation phase portrait in two-parameter space (g_{Ca}, g_{K}) is shown in Fig. 6(a). The solid lines $H1$ and $H2$ are threshold manifolds composed of Hopf bifurcation points. In the region left to $H1$ there are stable focus, while between $H1$ and $H2$ there are period one limited cycles. There exist other equilibrium states in the region right and lower to $H2$, which are not studied in the present paper.

We selected two representative points in g_{Ca}–g_{K} plane, $C1$(5.4, 10) and $C2$(7.4, 12), as shown in Fig. 6(a), to resemble two different cells. The $C1$ is located very close to the bifurcation boundary, thus, the stochastic ML model with $C1$ generates integer multiple oscillations, as shown in Fig. 6(b). In the delay coordinate trajectory of this oscillation (Fig. 6(c)), it is clearly seen that this trajectory is composed of

stochastic alternations between two orbits, one is a super-threshold action potential and the other is a sub-threshold oscillation around the focus. With the IAI defined as same as that in experiment, IAI series (Fig. 6(d)), IAI first return map (Fig. 6(e)), and IAI histogram distribution (Fig. 6(f)) from the modeling closely reproduce the characteristics of the experimental observation on single heart cells. Nonlinear prediction estimation also indicates a stochastic property for the simulated integer multiple oscillation.

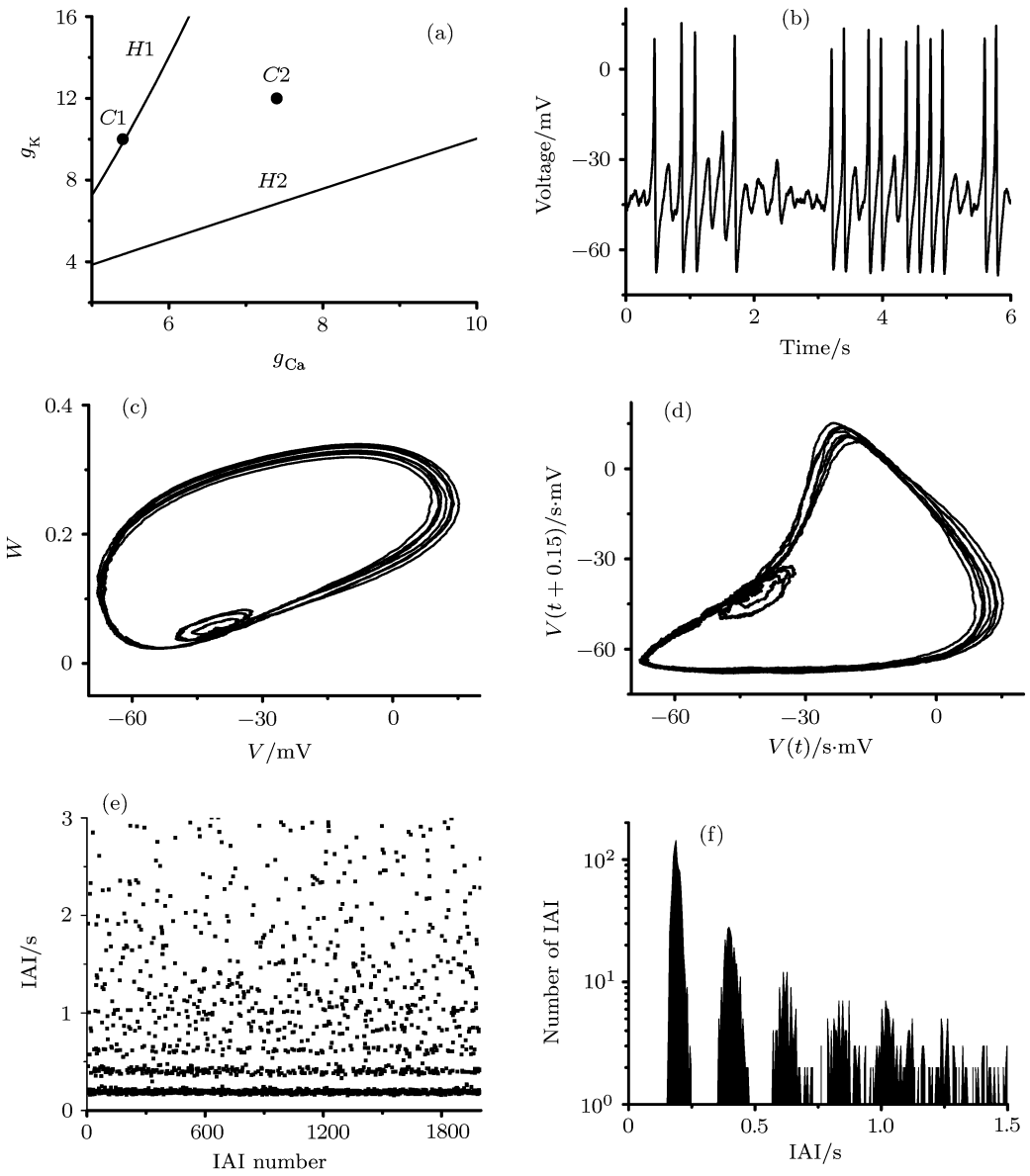


Fig. 6. The integer multiple oscillation generated by an ML cell with its g_{Ca} and g_K configured near to a Hopf bifurcation: (a) bifurcation diagram in g_{Ca}–g_K plane, showing the two representative points $C1$ and $C2$; (b) integer multiple oscillation of the model with $C1$ when $D = 0.02$; (c) the trajectories of this oscillation of $C1$ in V–W plane; (d) trajectory of this oscillation in delay coordinate portrait; (e) the IAI series of this oscillation; (f) the IAI histogram of this oscillation.

In contrast, since $C2$ is located between $H1$ and $H2$ and relatively far away from the bifurcations, the deterministic and stochastic models with $C2$ only manifest regular periodic oscillations in a large range of noise density.

In order to reveal the underpinning dynamics of the above simulation, we studied the bifurcation diagram with respect to injection current I in the deterministic ML model (with noise density $D = 0$) of $C1$. As shown in Fig. 7(a), there exists a sub-critical Hopf bifurcation point near $I = 0$ and a supercritical Hopf bifurcation point near $I = 160$. The subcritical Hopf bifurcation is in relevance to the present study. In stochastic ML model of $C1$ (with noise density $D = 0.02$), by adjusting the injection current I to simulate the different excitable states

or oscillations state, a series of oscillation patterns are induced, including sub-threshold oscillation (Fig. 7(b)), the integer multiple oscillation (Figs. 7(c)–7(e)), and regular super-threshold oscillation (Fig. 7(f)). These simulation results also predict that the integer multiple oscillations is an intermediate activities between resting and regular oscillations and induced by dynamic effect of noise.

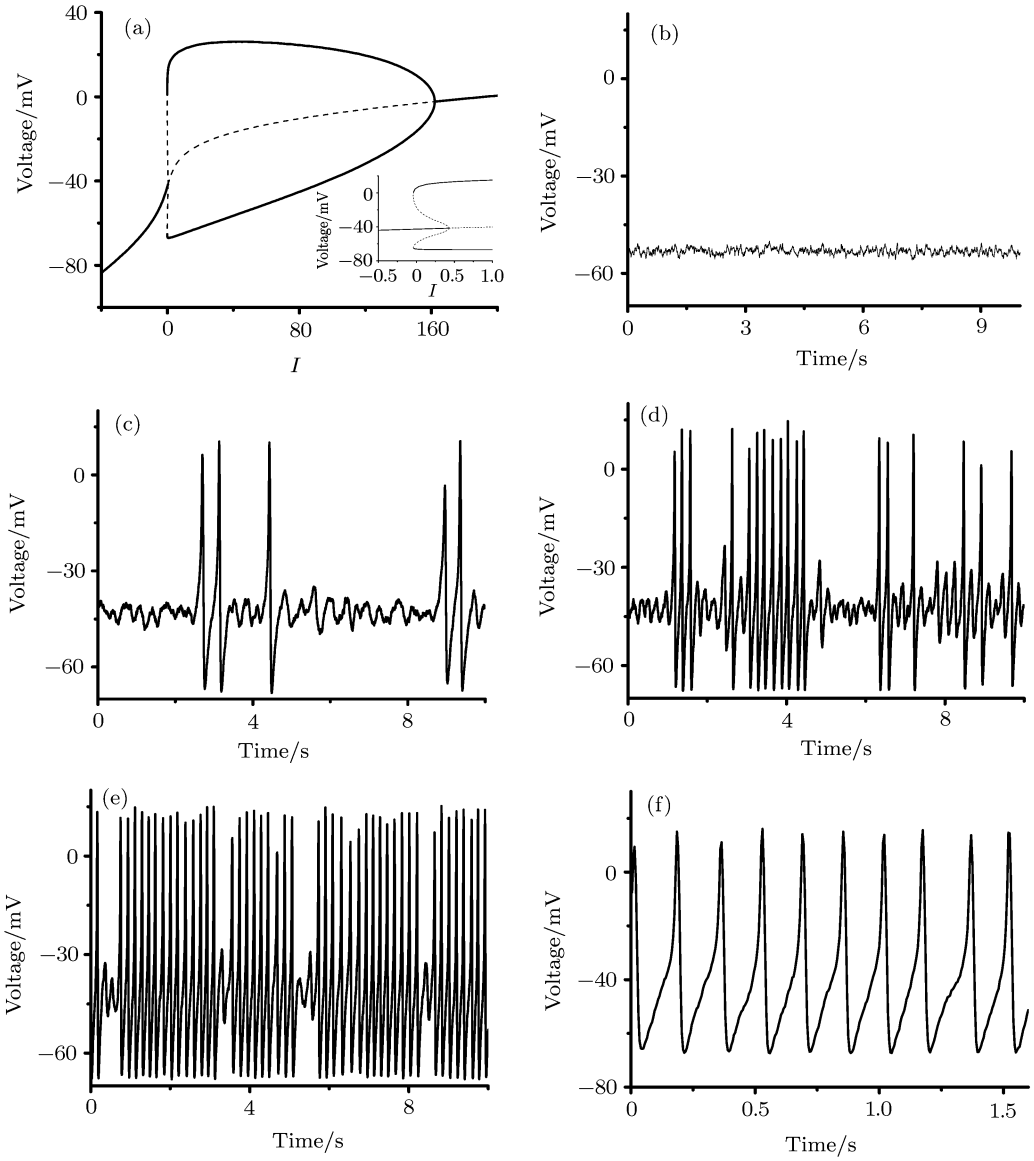


Fig. 7. (a) Bifurcation diagram of $C1$ with respect to I. (b) Sub-threshold oscillation when $I = -5$. (c) Integer multiple oscillation when $I = -0.1$. (d) Integer multiple oscillation when $I = 0.1$. (e) Integer multiple oscillation when $I = +0.432$. (f) Regular oscillation when $I = +1$.

6. Theoretical prediction for the integer multiple oscillations generated by heart-cell networks

To describe the heart-cell clusters employed in our present experiment, nearest-neighbour coupling and noise are considered to formulate network models composed of $N \times N$ cells as follows:

$$\begin{aligned} C\frac{\mathrm{d}V_{i,j}}{\mathrm{d}t} &= -g_{\mathrm{Ca}_{(i,j)}} m_{\infty_{(i,j)}}(V_{i,j} - V_{\mathrm{Ca}}) \\ &\quad - g_{\mathrm{K}_{(i,j)}}\omega(V_{i,j} - V_{\mathrm{K}}) \\ &\quad - g_{\mathrm{L}}(V_{i,j} - V_{\mathrm{L}}) + I_{c(i,j)}, \end{aligned} \tag{7}$$

$$\frac{\mathrm{d}\omega_{i,j}}{\mathrm{d}t} = \phi\frac{\omega_{\infty(i,j)} - \omega_{i,j}}{\tau_{\omega(i,j)}}, \tag{8}$$

where $(i,\ j)$ indicates location of each of the cells in this square lattice network with non-flux boundary condition. The $I_{c(i,j)}$ is the coupling current of the $(i,\ j)$-th cell. Expressions of $I_{c(i,j)}$ for boundary cells and those for inter-cells are different. Inter-cells, where $1 < i < N$ and $1 < j < N$, couples with 4 neighbours through $I_{c(i,j)} = g_{\rm c}(V_{i-1,j} + V_{i+1,j} + V_{i,j+1} + V_{i,j-1} - 4V_{i,j})$. Boundary cells couples with 3 neighbours through, for example, $I_{c(i,j)} = g_{\rm c}(V_{i+1,j} + V_{i,j+1} + V_{i,j-1} - 3V_{i,j})$ $(i = 1,\ 1 < j < N)$. Four corner-cells couples with 2 neighbours through, for example, $I_{c(i,j)} = g_{\rm c}(V_{i-1,j} + V_{i,j+1} - 2V_{i,j})$ $(i = N,\ j = 1)$.

To resemble the clusters used in our experiment, N is chosen as 4 while values of $g_{{\rm Ca}(i,j)}$ and $g_{{\rm K}(i,j)}$ are varied to reflect heterogeneities of the cells. In $g_{\rm Ca} - g_{\rm K}$ plane, we use ${\rm CL}(g_{\rm Ca}, g_{\rm K})$ to represent a cluster whose inclusive cells are configured around $((g_{\rm Ca}, g_{\rm K}))$. The heterogeneity of the cells within cluster CL is considered by bias from $(g_{\rm Ca}, g_{\rm K})$. The $(g_{{\rm Ca}(i,j)},\ g_{{\rm K}(i,j)})$, corresponding to the i,j cell in the CL is chosen as $(g_{\rm Ca}(1 + 0.1r_{i,j}), g_{\rm K}(1 + 0.1R_{i,j}))$, where $r_{i,j}$ and $R_{i,j}$ are random numbers between -1 and 1. Presuming very small scale $(N = 4)$ and nearest-neighbour connections of the clusters CL with parameters $(g_{{\rm Ca}(i,j)},$ $g_{{\rm K}(i,j)})$ (labeled as CL $(g_{\rm Ca},\ g_{\rm K})$), in what follows we employ two different clusters, CL1 $(g_{\rm Ca} = 5.4,$ $g_{\rm K} = 10)$ and CL2 $(g_{\rm Ca} = 7.4,\ g_{\rm K} = 12)$, to consider the effects of coupling strength and noise on synchronization in the clusters.

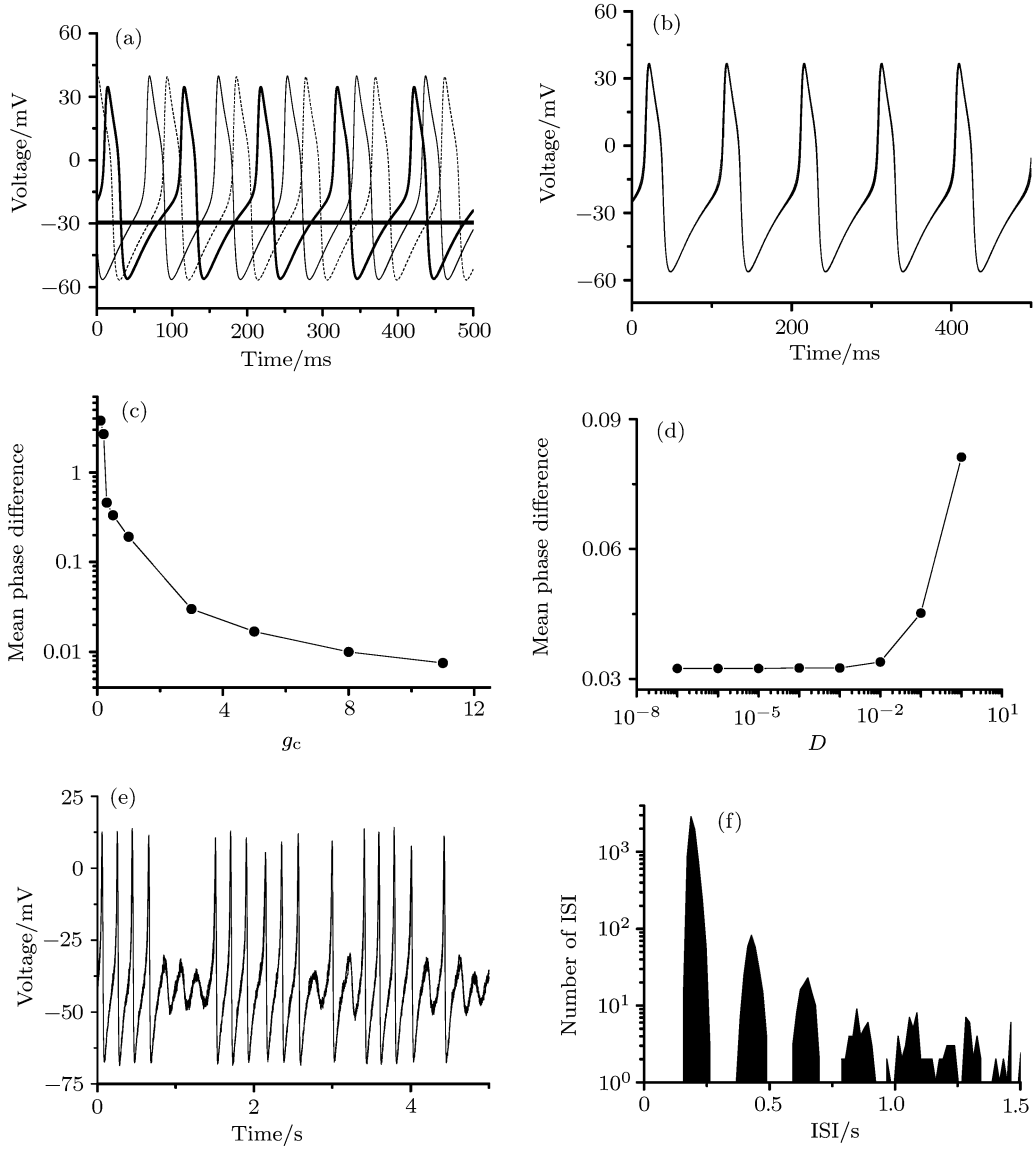


Fig. 8. (a) Spike trains of cluster CL1 when $g_{\rm c} = 0$. (b) Synchronous spike trains of cluster CL1 when $g_{\rm c} = 3$ and noise density $D = 0$. (c) Changes of mean phase-difference of cluster CL1 with respect to $g_{\rm c}$ when noise density $D = 0$. (d) Mean phase-difference of cluster CL1 with respect to noise density (D) when $g_{\rm c} = 3$. (e) Synchronous integer multiple oscillation of cluster CL1 when $g_{\rm c} = 3$ and $D = 0.12$. (f) IAI of CL1 when $g_{\rm c} = 3$ and $D = 0.12$.

Gaussian white noise $\xi_{i,j}(t)$ was introduced to Eq. (7) to form the stochastic network. The statistical properties of $\xi_{i,j}(t)$ is $\langle \xi_{i,j}(t) \rangle = 0$ and $\langle \xi_{i,j}(t)\xi_{m,n}(t') \rangle = 2D\delta(t-t')\delta_{i,j}\delta_{m,n}$. The equations of the deterministic and stochastic ML models and their networks were solved by Euler numerical integration method with integration time step being 0.1 s. Upstrokes of voltage reached the amplitude of 25.0 mV are counted as pulses.

We first consider the effect of coupling strength for CL1 with noise density fixed as zero. Increase of coupling strength results in synchronization of the heterogeneous cells in the two clusters. The mean value of phase-difference between the cells decreases exponentially with respect to linear increment of g_c. When $g_c = 0$, the voltage evolvement of the cells in CL1 is independent, as shown in Fig. 8(a). When $g_c = 3$ for CL1, voltage evolvement of the coupled cells became synchronous, as shown in Fig. 8(b). The exponential decrease in mean value of phase-difference of CL1 with respect to increase of g_c is shown in Fig. 8(c).

We then consider the effect of noise on synchronous oscillation in the cluster with fixed coupling strength ($g_c = 3$) for CL1. Elevation of the density of noise from zero to 1 imposes temperate disturbances on the synchronization between cells, causing slight increase in mean phase-difference. For CL1, the phase difference increased to about 0.08, as shown in Fig. 8(d).

We finally consider the synchronous integer multiple oscillations. Synchronous integer multiple oscillations appear only in simulation with CL1 network when noise density is larger than 0.06. An example of such oscillation with $D = 0.12$ is shown in Fig. 8(e). Comparing this oscillation with what simulated by using single cell model in previous sections, one can clearly see that the integer multiple oscillation also results from the effect of noise on synchronous cluster very near to a Hopf bifurcation boundary. This oscillation is induced by noise through dynamically driving the system to alternation between a super-threshold trajectory of a limited cycle and a sub-threshold trajectory around a focus. Exponentially decaying distribution in IAI histogram of this integer multiple oscillation (Fig. 8(f)) also indicates the stochastic nature of the alternation. NPE of the IAI series is nearly 1, suggesting that the IAI series may result from a stochastic dynamics (not shown here). The above numerical simulation and analysis very closely predict the experimental discovery on heart-cell clusters.

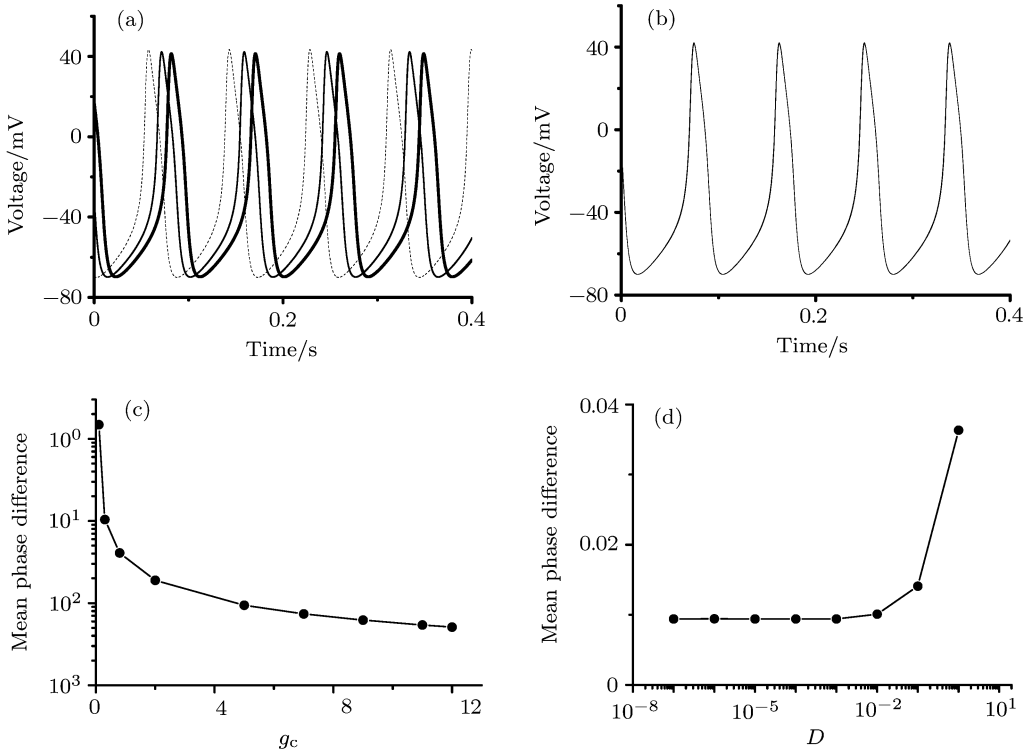


Fig. 9. (a) Spike trains of cluster CL2 when $g_c = 0$. (b) Synchronized spike trains of cluster CL2 when $g_c = 5$. (c) Changes of mean phase-difference of cluster CL2 with respect to g_c. (d) Mean phase-difference of cluster CL2 with respect to noise density (D).

For CL2, when $g_c = 0$, the voltage evolvement of the cells is independent and has period 1 rhythm, as shown in Fig. 9(a). The mean value of phase-difference of CL2 decreases with respect to increase of g_c, as shown in Fig. 9(c). For example, the period 1 rhythms become synchronous when $g_c = 5$, as shown in Fig. 9(b). When noise density increases, the phase-difference for CL2 with noise increases slightly, but the rhythm is also period 1, as shown in Fig. 9(d).

7. Discussion and conclusion

In this study, we observed the integer multiple oscillations in cultured heart-cell clusters in a series of particularly designed experiments and reproduced the observed phenomena from effects of noise on excitable or oscillating states near a Hopf bifurcation point. Simultaneous recordings of calcium oscillations in each of the inclusive cells indicate that the cells oscillate synchronously in a cluster. The seemingly complex integer multiple oscillations are estimated to be generated from a simple stochastic process, very similar to the behaviour of a double-well system under the drive of noise. Experimentation on single heart cells forming these clusters shows that the cells are heterogeneous in spontaneous oscillations. Some cells also exhibit such integer multiple oscillations while others exhibit regular rhythms. Current injection experiments reveal that the integer multiple oscillations have intermediate transient behaviours between resting and regular oscillation. Under ramp current injection the cells displays a transition from resting to incrementing sub-threshold oscillations, to integer multiple oscillation, and then to regular super-threshold excitations, indicating that a Hopf bifurcation dynamics of excitable system may reproduce the observed behaviours.

We hypothesized that the spontaneous active single heart cells are heterogeneous in their conductance configuration and therefore are dynamically located at different excitable or oscillatory states corresponding to different distances to the Hopf bifurcation point from resting to regular oscillation. Clusters formed by cells nearby the bifurcation point will manifest synchronous integer multiple oscillations under the drive of internal noise. By using a simple but explicit mathematical model[37] and its network, we considered the internal noise and heterogeneity according to previous biological data and then precisely reproduced the experimental observations on both single cell- and cluster-levels. In our theoretical analysis, the dynamic effects of noise and CR phenomenon, which incorporate and confirm the results of previous investigations,[20−24] further indicate important roles of noise in the function of the heart,[28,29] although the CR phenomenon is still remain to be completely confirmed in future experiments in beating activities of the heart. In summary, we are bound to reach a conclusion that interplay between noise and a Hopf bifurcation dynamics of the excitable system may result in the integer multiple oscillations in heart-cell clusters, in which, heterogeneity of the cells is a determinant intrinsic property.

The integer multiple oscillations observed in heart-cell clusters in the present study exhibit in appearance some similarity to a number of previous reported abnormal beating rhythms resulting from phase-locking or blockage mechanisms.[2,10,16,38] An important example of such abnormal rhythm is the ventricular beating rhythm of an individual with heart failure and frequent abnormal heartbeats. This abnormal ventricular beating rhythm appears to be irregular and also exhibits integer multiple and exponential decay characteristics in histograms of inter-ventricular time intervals. Theoretical analysis with a model consisting of two interacting oscillators with stochastic elements closely reproduces the stochastic property of the ventricular beating rhythm and reveals the effects of noise on generation of atrioventricular block.[38] We presented in this study a different example of the integer multiple oscillation rhythms and suggested a different mechanism, dynamic drive of noise on different cells near a Hopf bifurcation point, for generation of such abnormal oscillation at both cellular and cluster level. Effects of noise on a Hopf bifurcation and such induced integer multiple firing rhythms have already been studied in a number of neuronal systems and justified to be of physiological significance in neural coding.[20−24] The results of this study provide new examples of such oscillation rhythms in cardiac tissues and further imply the significance of bifurcation dynamics and noise in normal and abnormal cardiac rhythmgenesis.

A number of classical works have shown that heart cells can be induced to transit from regular oscillation to steady resting state and the dynamics of a Hopf bifurcation may underpin this transition.[1] In the case of a subcritical Hopf bifurcation, single pulse perturbation is able to annihilate the limited cycle oscillation by driving the system to the co-existing focus.[1,2] We observed in this study that a ramp current is able to induce a transition from resting to limited cycle oscillation. The sub-threshold oscillation appears between resting and limited cycle oscillation

implies that this transition is likely associated with a supercritical Hopf bifurcation. Some realistic mathematical models based on ionic conductance of heart cells, for instance the Beeler–Reuter model,[39] predict saddle-node bifurcations from resting to regular oscillations. One may conclude that the above difference might reflect heterogeneity of different heart-cells. The heterogeneity in oscillatory patterns as we observed in this study might represent biological variability in ionic conductance of the heart cells. In our simulation for integer multiple oscillations we only considered the differences in distance to the Hopf bifurcation point (corresponding to different excitable degrees) and expressed them by denoting varied values to the ionic conductance of the cells. Our consideration is partly motivated by biological data of heterogeneity of normal heart cells (see Ref. [40] and the references therein) and enlargement of this heterogeneity in pathological conditions such as early ischemia and heart failure.[41,42] The bifurcation dynamics in relevance to biological heterogeneity of heart cells still needs to be addressed in future works.

Whether the fluctuation caused by noise is essential or not in biological function is still contestable.[2] What we have to admit is that noise imposes good effects and bad effects in different circumstances. An example of the good is the improvement for detection of signals by neural tissues in the presence of suitable noise.[20−23] Effect of weak perturbation on resetting and annihilation of reentrant abnormal heartbeat is also an evidence of the good.[16] In contrast, noise might be able to annihilate regular heart beat by driving the system into a 'black hole', as in the above discussed case of a subcritical Hopf bifurcation.[1] We have shown in this paper that small cluster of heart cells under the drive of dynamic noise exhibits stochastic alternation between super- and sub-threshold oscillations. The appearance of this stochastic alternating rhythm is similar to some abnormal heart beat rhythms, such as what associated with sinus arrest. In the sinoatrial node, pacemaker cells assemble to clusters and oscillate synchronously. In aging heart or injured heart after early ischemia, sparsely occurred cell death through apoptosis or autophagy may result in enlargement of heterogeneity of the cells,[41,42] so as to shift the cluster nearby a bifurcation to rest. In this case noise may induce stochastic failures of pacemaking oscillation.

In addition, it is noticeable that the spatiotemporal patterns of $[Ca^{2+}]_i$ have had more and more attention,[4,30−32,43−53] because the important significance of calcium in the biological system including cardiac system.[4,30−32,43−52] When the space resolution of $[Ca^{2+}]_i$ is relatively low, waves including spiral wave can be discovered in the experiment or simulated in the theoretical model in large scale network composed of many cardiac cells or excitable media, related to cardiac arrhythmias or tachycardia,[4,30−32,43−45] has been one of the most important issues. The wave patterns are related to many factors such as the excitable degree of the media or network. When the space resolution is extra-high,[49] the spatiotemporal pattern of $[Ca^{2+}]_i$ can be recorded in a single cell, there is another important issue about calcium waves,[47−52] wherein calcium induced calcium release plays important roles.[47,48] When the space resolution of $[Ca^{2+}]_i$ is relative low and the coupling strength is high, the synchronized behaviours are exhibited in small scale heart-cell network, similar to the previous study about small scale network.[54] When the excitable degree of cells is different, the synchronized behaviours are different. If the behaviours of cells are nearby the Hopf bifurcation point from resting condition to period 1 rhythm in this paper and in Ref. [29], the synchronized complex rhythms are generated. If the behaviours of cells are far from the Hopf bifurcation point, the synchronized rhythm is period 1. The results about $[Ca^{2+}]_i$ in small scale network are the supplement to those of the large scale network[4,30−32,43−46] and single cells.[47−52]

References

[1] Glass L and Mackey M C 1988 *From Clock to Chaos: the Rhythms of Life* (Princeton: Princeton University Press) p. 1

[2] Glass L 2001 *Nature* **410** 277

[3] Clusin W T 2003 *Crit. Rev. Clin. Lab. Sci.* **40** 337

[4] González H, Nagai Y, Bub G, Glass L and Shrier A 2003 *BioSystems* **71** 71

[5] Kanakov O I, Osipov G V, Chan C K and Kurths J 2007 *Chaos* **17** 015111

[6] Ponard J G, Kondratyev A A and Kucera J P 2007 *Biophys. J.* **92** 3734

[7] Clay J R and DeHaan R L 1979 *Biophys. J.* **28** 377

[8] Michaels D C, Matyas E P and Jalife J 1987 *Circ. Res.* **61** 704

[9] Glass L, Guevara M R and Shrier A 1983 *Phyica* D **7** 89

[10] Guevara M R, Glass L and Shrier A 1981 *Science* **214** 1350

[11] Cai D, Winslow R L and Noble D 1994 *IEEE Trans. Biomed. Eng.* **41** 217

[12] Soen Y, Cohen N, Lipson D and Braun E 1999 *Phys. Rev. Lett.* **82** 3556

[13] Yamauchi Y, Harada A and Kawahara K 2002 *Biol. Cybern.* **86** 147

[14] Jalife J 1984 *J. Physiol.* **356** 221

[15] Aihara R and Hara M 2005 *Biophys. Chem.* **116** 33

[16] Glass L and Josephson M E 1995 *Phys. Rev. Lett.* **75** 2059

[17] Jung P, Cornell-Bell A, Moss F, Kadar S, Wang J and Showalter K 1998 *Chaos* **8** 567

[18] Zheng Z G 2004 *Spatiotemporal Dynamics and Collective Behaviours in Coupled System* (Beijing: Higher Education Press) p. 175

[19] Lindner B, García-Ojalvo J, Neiman A and Schimansky-Geier L 2004 *Phys. Rep.* **392** 321

[20] Braun H A, Wissing H, Schäfer K and Hirsch M C 1994 *Nature* **367** 270

[21] Longtin A, Bulsara A and Moss F 1991 *Phys. Rev. Lett.* **67** 656

[22] Gu H G, Ren W, Lu Q S, Wu S G, Yang M H and Chen W J 2001 *Phys. Lett.* A **285** 63

[23] Gu H G, Yang M H, Li L, Liu Z Q and Ren W 2002 *NeuroReport* **13** 1657

[24] Yang M H, Li L, Liu Z Q, Xu Y L, Liu H J, Gu H G and Ren W 2009 *Int. J. Bifur. Chaos* **19** 453

[25] Benzi R, Sutera A and Vulpiani A 1981 *J. Phys.* A **14** L453

[26] Hu G, Ditzinger T, Ning C Z and Haken H 1993 *Phys. Rev. Lett.* **71** 807

[27] Lerma C, Krogh-Madsen T, Guevara M R and Glass L 2007 *J. Stat. Phys.* **128** 347

[28] Kim M Y, Aguilar M, Hodge A, Vigmond E, Shrier A and Glass L 2009 *Phys. Rev. Lett.* **103** 058101

[29] Zhang N, Zhang H M, Liu Z Q, Ding X L, Yang M H, Gu H G and Ren W 2009 *Chin. Phys. Lett.* **26** 110501

[30] Bub G, Glass L, Publicover N G and Shrier A 1998 *Proc. Natl. Acad. Sci. USA* **95** 10283.

[31] Bub G, Shrier A and Glass L 2002 *Phys. Rev. Lett.* **88** 058101

[32] Bub G, Tateno K, Shrier A and Glass L 2003 *J. Cardiovasc. Electr.* **14** 229

[33] Liu H J, Liu Z Q, Gu H G, Yang M H, Li L and Ren W 2006 *Acta Biophys. Sin.* **22** 441 (in Chinese)

[34] Demir S S, Clark J W, Murphey C R and Giles W R 1994 *Am. J. Physiol. Cell Physiol.* **266** C832

[35] Kurata Y, Hisatome I, Imanishi S and Shibamoto T 2002 *Am. J. Physiol Heart Circ. Physiol.* **283** H2074

[36] FitzHugh R 1961 *Biophys. J.* **1** 445

[37] Morris C and Lecar H 1981 *Biophys. J.* **35** 193

[38] Schulte-Frohlinde V, Ashkenazy Y, Ivanov P C, Glass L, Goldberger A L and Stanley H E 2001 *Phys. Rev. Lett.* **87** 068104

[39] Beeler G W and Reuter H 1977 *J. Physiol.* **268** 177

[40] Peter K 2003 *Circ. Res.* **93** 381

[41] Takemura G, Miyata S, Kawase Y, Okada H, Maruyama R and Fujiwara H 2006 *Autophagy* **2** 212

[42] Dimmeler S and Leri A 2008 *Circ. Res.* **106** 1319

[43] Liu S Q, Lu Q S and Wang Q 1998 *Acta Phys. Sin.* **47** 1057 (in Chinese)

[44] Ma J, Jin W Y, Li Y L and Chen Y 2007 *Acta Phys. Sin.* **56** 2456 (in Chinese)

[45] Yin X Z and Liu Y 2008 *Acta Phys. Sin.* **57** 6844 (in Chinese)

[46] Wilkins M and Sneyd J 1998 *J. Theor. Biol.* **191** 299

[47] Shi X M and Liu Z R 2005 *Chin. Phys. Lett.* **22** 3206

[48] Orchard C H, Mustafa M R and White E 1995 *Chaos, Solitons and Fractals* **5** 447

[49] Bai Y Q, Tang A H, Wang S Q and Zhu X 2007 *Acta Phys. Sin.* **56** 3607 (in Chinese)

[50] Tang A H and Wang S Q 2008 *Acta Phys. Sin. Prog. Biochem. Biophys.* **35** 892

[51] Cheng H, Lederer W J and Cannell M B 1993 *Science* **262** 740

[52] Davidenko J M, Pertsov A V, Salomonsz R, Baxter W and Jalife J 1992 *Nature* **355** 349

[53] Wang B H, Lu Q S, Lü S J and Lang X F 2009 *Chin. Phys.* B **18** 872

[54] Shi X and Lu Q S 2005 *Chin. Phys.* **14** 77